Coulomb drag between quantum wires in a magnetic field

H. C. Tso and P. Vasilopoulos
Department of Physics, Concordia University, 1455 de Maisonneuve Boulevard West, Montréal, Québec, Canada H3G 1M8
(Received 5 March 1991; revised manuscript received 29 May 1991)

Momentum transfer between two quasi-one-dimensional electron gases, mediated by the Coulomb interaction, is considered in the presence of a magnetic field normal to the plane of the gases. The lateral confinement is assumed to be parabolic. Impurity scattering (screened) and electron-electron interaction are treated self-consistently within the random-phase approximation. The current response is evaluated from the derived momentum-balance equations, which involve the nonequilibrium electron polarizability, in conjunction with a drifted-temperature model for the polarizability. An applied current driven through either of the gases, whose centers are separated by a distance a, induces a contactless current in the other gas about 10^5 times smaller and in direct analogy with the zero-magnetic-field observations of Solomon *et al.* Both the applied and the induced current exhibit Shubnikov–de Haas oscillations. The applied current increases slightly with a and saturates at a finite value. In contrast, the induced current decreases approximately as a^{-2} for a much larger than the wire width.

I. INTRODUCTION

Electron-electron interaction between well-separated electron-gas layers has already been considered.[1] The interaction has been predicted to lead to momentum and/or energy transfer between the electron gases and thus to modify, e.g., the transport properties of one of them when an electric field is applied to the other. This has been confirmed recently by the observation[2] of an induced, contactless, current in a two-dimensional (2D) electron gas, separated by a distance of 300 Å from a (semi-infinite) three-dimensional (3D) gas when a current was driven through the latter or vice versa. The subsequent interpretation[3] of this observation made use of the above-mentioned energy and momentum transfer.

All relevant works[1–3] of which we are aware are valid in the absence of a magnetic field. It is of interest, of course, to examine more closely how the latter influences momentum and/or energy transfer between, e.g., two electron gases. This is the subject of this paper. The geometry that we chose is that of two quantum wires (along the x axis) whose centers are separated by a distance a along the y axis and in the presence of a perpendicular magnetic field $\mathbf{B} = B\hat{z}$. This choice was motivated by the increasing interest that quantum wires have attracted in recent years after the observation of quantum size effects such as the oscillatory behavior of the conductivity, as function of the impurity density,[4] the quenching of the Hall effect,[5] etc. An additional reason is the quantitative assessment of the changes in screening, studied self-consistently, when a magnetic field is present and the dimensionality is reduced. In the next section, we present the formalism and in Sec. III numerical results and discussion. A summary follows in the last section.

II. THE FORMALISM

A. Model for coupled quantum wires

The many-body Hamiltonian $H(t_1)$ is given as

$$H(t_1) = H_\alpha(t_1) + H_\beta(t_1) + H_i(t_1) + H_{\alpha\beta}(t_1), \quad (1)$$

where

$$H_\gamma(t_1) = \int d\mathbf{r}_1\ \hat{\Psi}^\dagger_\gamma(1^+)h_\gamma(1)\hat{\Psi}_\gamma(1) + \sum_a \int d\mathbf{r}_1\ v_i(\mathbf{r}_1-\mathbf{r}_a)\ \hat{\Psi}^\dagger_\gamma(1^+)\hat{\Psi}_\gamma(1) + \tfrac{1}{2}\int d\mathbf{r}_1 \int d\mathbf{r}_2\ \hat{\Psi}^\dagger_\gamma(1^+)\hat{\Psi}^\dagger_\gamma(\mathbf{r}_2,t_1^+) \times v(\mathbf{r}_1-\mathbf{r}_2)\hat{\Psi}_\gamma(\mathbf{r}_2,t_1)\hat{\Psi}_\gamma(1)\ , \quad (2)$$

$$H_{\alpha\beta}(t_1) = \int d\mathbf{r}_1 \int d\mathbf{r}_2\ \hat{\Psi}^\dagger_\alpha(\mathbf{r}_2,t_1^+)\hat{\Psi}_\alpha(\mathbf{r}_2,t_1) \times v(\mathbf{r}_1-\mathbf{r}_2)\hat{\Psi}^\dagger_\beta(1^+)\hat{\Psi}_\beta(1)\ , \quad (3)$$

and γ ($=\alpha$ or β) is the wire index. Here $v(\mathbf{r}_1-\mathbf{r}_2) = \bar{e}^2/|\mathbf{r}_1-\mathbf{r}_2|$ is the bare Coulomb interaction with $\bar{e}^2 = e^2/\epsilon_\infty$ and ϵ_∞ is the high-frequency dielectric constant. $H_i(t)$ is the impurity Hamiltonian, $v_i(\mathbf{r}_1-\mathbf{r}_a)$ is the bare-electron–impurity interaction taken to be Coulombic, with $\mathbf{r}_1$ and $\mathbf{r}_a$ being the positions of the electron and of the impurity, respectively; $\hat{\Psi}_\alpha(1)$ [$\hat{\Psi}_\beta(1)$] and $\hat{\Psi}^\dagger_\alpha(1)$ [$\hat{\Psi}^\dagger_\beta(1)$] are the field operators pertaining to the electron system in the α (β) wire. The last term of Eq. (1), $H_{\alpha\beta}(t_1)$, as given by Eq. (3) is the Hamiltonian of the

interaction between electrons in wire α and electrons in wire β.

We model the lateral confinement with a parabolic (confining) potential of frequency Ω, $V_y = m^*\Omega^2 y^2/2$, and for simplicity we take the thickness L_z to be zero. In this case,

$$h_\gamma(1) = [\, -i\nabla_1 - \bar{e}\mathbf{A}_\gamma(\mathbf{r}_1,t_1)\,]^2/2m^* + m^*\Omega^2 y^2/2 \tag{4}$$

is the one-electron Hamiltonian of the γ ($\gamma = \alpha$ or β) wire in the presence of an external magnetic field $\mathbf{B} = B\hat{\mathbf{z}}$ and of an electric field $\mathbf{E}(\mathbf{r}) = E\hat{\mathbf{x}}$ applied only in the α wire whose center is located at $y = a/2$ and whose width is w. The vector potential $\mathbf{A}_\gamma(\mathbf{r},t)$ is thus given by

$$\mathbf{A}_\gamma(\mathbf{r}_1,t_1) = -[\,(t_1 - t_0)\,E_\gamma + B\,y_1\,]\hat{\mathbf{x}}, \tag{5}$$

where $E_\alpha = E$ and $E_\beta = 0$. We assume that the α and β wires are identical. The one-electron eigenfunction for wire α, $\psi^\alpha_{n,k_x}(\mathbf{r})$, and the eigenvalue ε_{n,k_x} for zero electric field are

$$\psi^\alpha_{n,k_x}(\mathbf{r}) = \phi_n(y - y_0(k_x) - a/2)e^{ik_x x}/\sqrt{L}\,, \tag{6}$$

$$\varepsilon_{n,k_x} = (n + \tfrac{1}{2})\hbar\tilde{\omega} + \hbar^2 k_x^2/2\tilde{m}, \tag{7}$$

respectively; for wire β the eigenfunction is given by Eq. (6) with $-a/2$ replaced by $a/2$ and the eigenvalue is the same; n is the Landau-level index, k_x is the wave vector in the x direction, m^* is the conduction-band mass, $\tilde{\omega} = \sqrt{\omega_c^2 + \Omega^2}$, $\tilde{m} = m^*\tilde{\omega}^2/\Omega^2$, $y_0(k_x) = \tilde{b}\,\tilde{l}_B^2 k_x$ with $\tilde{b} = \omega_c/\tilde{\omega}$ and $\tilde{l}_B^2 = \hbar/m^*\tilde{\omega}$. $\phi_n(y)$ are the well-known harmonic-oscillator wave functions. The main difference of Eq. (7) from the corresponding expression for a wide 2D channel ($\Omega = 0$) is the absence of the term $\hbar^2 k_x^2/2\tilde{m}$ in the latter: that is, the presence of the confining potential ($\Omega \neq 0$) lifts the k_x degeneracy of the 2D energy levels and the electrons appear heavier since $\tilde{m} > m^*$. As for the wire width w it is related to the confining frequency Ω and the 1D electron density n^{1D} approximately by[6]

$$w = 2\pi\sqrt{n^{1D}}\,(2\hbar/3\pi m^*\Omega)^{2/3}. \tag{8}$$

We should bear in mind that the Hamiltonian in Eq. (1) is valid only if particle exchange between wires induced either by tunneling or any other nonlocal perturbations, such as $v(\mathbf{r}_1 - \mathbf{r}_2)$ and $v_i(\mathbf{r}_1 - \mathbf{r}_a)$, is ignored. This neglect of particle exchange and of tunneling is justified for relatively large separations between the wires, $a \geq 70$ Å; we have made it in order to better assess the influence of the Coulomb coupling between the wires.

B. Momentum-balance equations

The momentum-balance equations for electrons in different wires are obtained by applying the operators $\lim_{2\to 1^+}\{-(\bar{e}/2m^*)[\nabla_1 - \nabla_2 - 2i\bar{e}\mathbf{A}_\alpha(\mathbf{r}_1,t_1)]\}$ and $\lim_{2\to 1^+}\{-(\bar{e}/2m^*)[\nabla_1 - \nabla_2 - 2i\bar{e}\mathbf{A}_\beta(\mathbf{r}_1,t_1)]\}$ to the equation of motion of the thermodynamic electron Green's functions $g^\alpha_<(1;2)$ and $g^\beta_<(1;2)$, respectively, defined in terms of the field operators $\Psi_\alpha(1)$, $\Psi_\beta(1)$, $\Psi^\dagger_\alpha(1)$, $\Psi^\dagger_\beta(1)$, and of the equilibrium density matrix ρ_0 as[7]

$$g^\gamma_<(1;2) \equiv i\,\mathrm{Tr}[\rho_0\Psi^\dagger_\gamma(2)\Psi_\gamma(1)]/\mathrm{Tr}(\rho_0), \tag{9}$$

and by subtracting the results of the operation from their adjoint counterparts. In the shielded potential approximation[8,9] which neglects vertex corrections in the electron-impurity and electron-electron interaction, the momentum-balance equations for electrons in terms of their nonequilibrium number polarizabilities $\Pi^\gamma_{\gtrless}$ (see below) and of the shielded interaction $\tilde{v}^\gamma_{\alpha\beta}$ is

$$-\frac{m^*}{\bar{e}}\frac{\partial \mathbf{j}_\alpha(t_1)}{\partial t_1} + \bar{e}n^{1D}_\alpha\mathbf{E} + \mathbf{j}_\alpha(t_1)\times\mathbf{B} - \bar{e}\,n^{1D}_\alpha\mathbf{E}^\alpha_H(t_1) = \mathbf{J}^{\alpha\beta}, \tag{10}$$

$$-\frac{m^*}{\bar{e}}\frac{\partial \mathbf{j}_\beta(t_1)}{\partial t_1} + \mathbf{j}_\beta(t_1)\times\mathbf{B} - \bar{e}n^{1D}_\beta\mathbf{E}^\beta_H(t_1) = \mathbf{J}^{\beta\alpha}, \tag{11}$$

where

$$\mathbf{J}^{\alpha\beta} = \int dy_1\int dz_1\int_{t_0}^{t_1} d(3)[\,\Pi^\alpha_>(1;3)\,\nabla_1\tilde{v}^\alpha_{\alpha\beta\,>}(1;3) - \Pi^\alpha_<(1;3)\nabla_1\tilde{v}^\alpha_{\alpha\beta\,<}(1;3)\,] \tag{12}$$

and γ is either α or β. The Hall field $\mathbf{E}^\gamma_H$ is given by

$$\mathbf{E}^\gamma_H = i\int dy_1\int dz_1\frac{1}{4m^*\,n^{1D}_\gamma}\nabla_1\cdot\{[\nabla_1 - \nabla_2 - 2i\bar{e}\mathbf{A}_\gamma(1)][\nabla_1 - \nabla_2 - 2i\bar{e}\mathbf{A}_\gamma(1)]g^\gamma_<(1;2)\}_{2=1^+}, \tag{13}$$

and $\mathbf{j}_\gamma$ and n^{1D}_γ are the 1D current and electron densities, respectively. In the above equation, $\Pi^\gamma_{\gtrless}(1;3)$ is the fluctuation of the electron density at space-time point $(\mathbf{r}_1,t_1)$ with respect to a change of the effective potential at space-time point $(\mathbf{r}_3,t_3)$ and $\tilde{v}_\gamma(1;3)$ is just the nonlocal shielded interaction between space-time points $(\mathbf{r}_1,t_1)$ and $(\mathbf{r}_3,t_3)$. Furthermore, the limits of integration on y_1 and z_1 are taken within the wire and phonon scattering is neglected for very low temperatures. The four-dimensional integration is defined as $\int_{t_0}^{t_1} d(3) \equiv \int_{t_0}^{t_1} dt_3 \int_{\text{all space}} d\mathbf{r}_3$, and the shielded interaction[10] is given by

$$\tilde{v}^\gamma_{\alpha\beta\,\gtrless}(1;2) = \int_{-\infty}^{\infty} d(3)\int_{-\infty}^{\infty} d(4)\,\bar{v}^\gamma_{i\,+}(1;3)\,n_i^{2D}\delta(\mathbf{x}_3 - \mathbf{x}_4)\,\bar{v}^\gamma_{i\,-}(4;2)\delta(z_3) + \int_{-\infty}^{\infty} d(3)\int_{-\infty}^{\infty} d(4)\bar{v}_+(1;3)\,\Pi^\alpha_{\gtrless}(3;4)\bar{v}_-(4;2) + \int_{-\infty}^{\infty} d(3)\int_{-\infty}^{\infty} d(4)\bar{v}_+(1;3)\,\Pi^\beta_{\gtrless}(3;4)\bar{v}_-(4;2). \tag{14}$$

In Eq. (14), n_i^{2D} is the 2D density of impurities located at $z = 0$. Furthermore, the retarded (advanced) screened electron-impurity interaction $\bar{v}_i^{\gamma}{}_+$ ($\bar{v}_i^{\gamma}{}_-$) and screened Coulomb interaction $\bar{v}_+$ ($\bar{v}_-$) are related to the retarded (advanced) inverse dielectric function K_+ (K_-) by the following equations:

$$\bar{v}_i^{\gamma}{}_+(1;2) = \int_{-\infty}^{\infty} d(3)\ K_+(1;3)v_i^{\gamma}{}_+'(3;2)\ , \tag{15}$$

$$\bar{v}_i^{\gamma}{}_-(1;2) = \int_{-\infty}^{\infty} d(3)\ K_-(3;2)v_i^{\gamma}{}_-'(1;3)\ , \tag{16}$$

$$\bar{v}_+(1;2) = \int_{-\infty}^{\infty} d(3)\ K_+(1;3)\delta(t_3 - t_2)v(\mathbf{r}_3 - \mathbf{r}_2)\ , \tag{17}$$

$$\bar{v}_-(1;2) = \int_{-\infty}^{\infty} d(3)\ K_-(3;2)v(\mathbf{r}_1 - \mathbf{r}_3)\delta(t_1 - t_3) \tag{18}$$

with

$$v_i^{\gamma}{}_{\pm}'(1;2) = v_i(\mathbf{r}_1 - \mathbf{r}_2)\delta(t_1 - t_2) - 2\int_{-\infty}^{\infty} d(3)\int_{-\infty}^{\infty} d(4)v(\mathbf{r}_1 - \mathbf{r}_3)\delta(t_1 - t_3)\Pi_{\pm}^{\bar{\gamma}\ (0)}(3;4)\delta(t_4 - t_2)v_i(\mathbf{r}_4 - \mathbf{r}_2). \tag{19}$$

In Eq. (19), $\bar{\gamma} = \beta$ for $\gamma = \alpha$ and $\bar{\gamma} = \alpha$ for $\gamma = \beta$. As shown in Eqs. (15), (16), and (19), the bare electron-impurity interaction is polarized by electrons in the other wire and screened by electrons in both wires. However, the bare Coulomb interaction is screened by electrons in both wires. No additional polarization from electrons in another wire is involved except screening.

C. Equilibrium inverse dielectric function

To determine the inverse of the dielectric function $\epsilon_{\pm}(q_x;\boldsymbol{\rho}_1,\boldsymbol{\rho}_2;\omega)$, of the system of the two wires in 3D (three-dimensional) space ($\boldsymbol{\rho}_1 = y_1\hat{\mathbf{j}} + z_1\hat{\mathbf{k}}$, $\boldsymbol{\rho} = \boldsymbol{\rho}_1 - \boldsymbol{\rho}_2$), we employ the inversion condition,

$$\int d\boldsymbol{\rho}_3\ \epsilon_{\pm}(q_x,\boldsymbol{\rho}_1,\boldsymbol{\rho}_3;\omega)K_{\pm}(q_x,\boldsymbol{\rho}_3,\boldsymbol{\rho}_2;\omega)\ = \delta(\boldsymbol{\rho})\ . \tag{20}$$

In random-phase approximation (RPA), the dielectric function can be written as

$$\epsilon_{\pm}(q_x,\boldsymbol{\rho}_1,\boldsymbol{\rho}_2;\omega) = \delta(\boldsymbol{\rho}) + \int d\boldsymbol{\rho}_3\ v(q_x;\boldsymbol{\rho}_1 - \boldsymbol{\rho}_3) \times R_{\pm}(q_x;\boldsymbol{\rho}_3,\boldsymbol{\rho}_2;\omega), \tag{21}$$

where

$$R_{\pm}(q_x;\boldsymbol{\rho}_1,\boldsymbol{\rho}_2;\omega) \simeq -\delta(z_1)\delta(z_2)[\,\delta(y_1^-)\delta(y_2^-)\Pi_{\pm}^{\alpha} + \delta(y_1^+)\delta(y_2^+)\Pi_{\pm}^{\beta}], \tag{22}$$

$$y_i^{\pm} = y_i \pm a/2,\quad i = 1,2\ ,\ \Pi_{\pm}^{\gamma} \equiv \Pi_{\pm}^{\gamma(0)}(q_x;\omega).$$

Furthermore,

$$\Pi_{\pm}^{\gamma\ (0)}(q_x;\omega) = 2\sum_{n,m}\int \frac{dk_x}{2\pi} C_{n,m}(q_x)\frac{f_{\gamma}(\varepsilon_{n,k_x}) - f_{\gamma}(\varepsilon_{m,k_x-q_x})}{\omega + \varepsilon_{n,k_x} - \varepsilon_{m,k_x-q_x} \pm i0^+} \equiv \Pi_{\pm}\ , \tag{23}$$

$$C_{n,n+m}(q_x) = \int dy_3 \int dy_4\ \phi_n^*(y_3^{\pm} - y_0(k_x))\phi_{n+m}(y_3^{\pm} - y_0(k_x - q_x))\phi_{n+m}^*(y_4^{\pm} - y_0(k_x - q_x))\phi_n(y_4^{\pm} - y_0(k_x)) = [n!/(n+m)!]u^m e^{-u}[L_n^m(u)]^2, \tag{24}$$

and

$$v(q_x;\boldsymbol{\rho}) = 2\tilde{e}^2 K_0(|q_x|\rho)\ . \tag{25}$$

Here $u = q_x^2\tilde{l}^2/2$, $L_n^m(u)$ is a Laguerre polynomial, and $K_0(x)$ is the zeroth-order modified Bessel function. The upper signs on the right-hand side of Eq. (24) refer to $\gamma = \beta$ and the lower ones to $\gamma = \alpha$. Note that the retarded (advanced) equilibrium [indicated by superscript (0)] number polarizability $\Pi_+^{\gamma\ (0)}$ ($\Pi_-^{\gamma\ (0)}$) relates to its greater (>) and lesser (<) counterparts by

$$\Pi_{\pm}^{\gamma\ (0)}(1;2) = \pm\,\eta_{\pm}(t_1 - t_2)\,[\Pi_>^{\gamma\ (0)}(1;2) - \Pi_<^{\gamma\ (0)}(1;2)]\ , \tag{26}$$

with $\eta_+(x)$ as the Heaviside step function and $\eta_-(x) \equiv 1 - \eta_+(x)$. To remove the divergence of the 1D Fourier transform of the Coulomb potential, $v(q_x;\boldsymbol{\rho})$, at either $q_x \to 0$ or $\rho \to 0$, we adopt the lower bound for q_x and ρ as q_c and $w/2$, respectively, discussed in Ref. 11, so that

$$v(q_x;\boldsymbol{\rho}) \simeq 2e^2 K_0(|q_x|\rho)\ \eta_+(|q_x|\rho - q_c w/2) + 2e^2 K_0(q_c w/2)\ \eta_-(|q_x|\rho - q_c w/2)\ . \tag{27}$$

Thus the solution of Eq. (20), in RPA, is

$$K_{\pm}(q_x;\boldsymbol{\rho}_1,\boldsymbol{\rho}_2;\omega) - \delta(\boldsymbol{\rho}) \simeq \sum_{i=1}^{2} v(q_x;\boldsymbol{\rho}_1 - \tfrac{1}{2}(-1)^i a\hat{\mathbf{y}}) \times \Pi_{\pm}(q_x;\omega)I_{i\ \pm}(q_x;\boldsymbol{\rho}_2;\omega), \tag{28}$$

with

$$I_{1\,\pm}(q_x;\rho_2;\omega) = I_{i\,\pm}(q_x;\rho_2;\omega)|_{i=1} \equiv K_{\pm}(q_x;\tfrac{1}{2}(-1)^i a\hat{\mathbf{y}},\rho_2;\omega)|_{i=1}$$
$$= \frac{\delta(z_2)}{\epsilon_{\pm}(q_x;\omega)}\{\delta(y_2^+) - [v(q_x;w)\delta(y_2^+) + v(q_x;a)\delta(y_2^-)]\Pi_{\pm}\}, \tag{29}$$

$$\epsilon_{\pm}(q_x;\omega) = [1 - v(q_x;w)\Pi_{\pm}^{\alpha}][1 - v(q_x;w)\Pi_{\pm}^{\beta}] - v(q_x;a)\Pi_{\pm}^{\alpha}v(q_x;a)\Pi_{\pm}^{\beta}\ . \tag{30}$$

We obtain $I_{2\,\pm}(q_x;\rho_2;\omega)$ from $I_{1\,\pm}(q_x;\rho_2;\omega)$ with the changes $y_2^+ \to y_2^-$ and $y_2^- \to y_2^+$. For $a \gg w$, Eq. (27) shows that the dielectric function $\varepsilon_{\pm}(\cdots)$ varies approximately as a, cf. Sec. III.

D. Expression for the conductivity

For transport along the α wire, we substitute $\tilde{v}_{\alpha}^{\gtrless}$ obtained from Eq. (14) into Eq. (10). The third term in Eq. (14), which leads to the frictional force due to the electron-electron scattering within the α wire, vanishes because of the symmetry property of $\Pi_{\lessgtr}^{\gamma}(1;2)$ [$\Pi_{\gtrless}^{\gamma}(1;2) = \Pi_{\gtrless}^{\gamma}(2;1)$]. However, the first term and the second term in Eq. (14) which lead to the frictional force due to electron-impurity scattering and the frictional force due to the electron-electron scattering between the two wires, are finite. To close Eqs. (10) and (11), we employ the drifted-temperature model and introduce drift velocities v_d^{α} and v_d^{β} related to the current densities along the α and β wires by $\mathbf{j}_{\gamma} = n^{1\mathrm{D}}\,\bar{e}\,v_d^{\gamma}\,\hat{\mathbf{x}}$ so that the 1D Fourier transform of the *nonequilibrium* number polarizabilities $\Pi_{\gtrless}^{\gamma}$ (without vertex corrections and in the weak-scattering limit) can be expressed, in the steady state, as

$$\Pi_{>}^{\gamma}(q_x;t_1,t_2)$$
$$= -2i\sum_{n,m,k_x} C_{n,m}(q_x)\, e^{-i(\varepsilon_{n,k_x}-\varepsilon_{m,k_x-q_x}-q_x v_d^{\gamma})(t_1-t_2)}$$
$$\times[\,1 - f_{\gamma}(\varepsilon_{n,k_x})\,]\, f_{\gamma}(\varepsilon_{m,k_x-q_x}). \tag{31}$$

In the above equation, $f_{\gamma}(\varepsilon_{n,k_x})$ is the Fermi-Dirac distribution function at the lattice temperature. We have assumed that the electric field is not strong enough to heat up the electrons. For $\Pi_{<}^{\gamma}(\cdots)$ we obtain Eq. (31) with the Fermi-Dirac factors interchanged. Furthermore, the shielded interaction is of the form $\int d\mathbf{x}_3 \int d\mathbf{x}_4 u(1;3)\Pi_{>}^{\gamma}(3;4)w(4;2)$ according to the drifted-temperature model in the steady state, and reduces to

$$-2i\sum_{q_x,k_x} e^{iq_x(x_1-x_2)}u(q_x;t_1-t_3)e^{-iq_x v_d^{\gamma}[t_1-t_2-2(t_3-t_4)]}w(q_x;t_4-t_2)$$
$$\times\sum_{n,m} C_{n,m}(q_x)e^{-i(\varepsilon_{n,k_x}-\varepsilon_{m,k_x-q_x})(t_3-t_4)}[1 - f_{\gamma}(\varepsilon_{n,k_x})]f_{\gamma}(\varepsilon_{m,k_x-q_x}) \tag{32}$$

for any equilibrium nonlocal (both in time and space) interactions $u(1;2)$ and $w(1;2)$ which are $\bar{v}_{\pm}(1;2)$ and $\bar{v}_{i\,\pm}^{\gamma}(1;2)$ in our case. Thus, we obtain the frictional force acting on the electron system in wire α, per unit mass and per unit length, due to impurity scattering as

$$F_{\alpha i} = \frac{2\,n_i^{2\mathrm{D}}}{m^*}\sum_{q_x}|\bar{v}_i^{\alpha}(q_x;\omega)|^2_{\omega=0}q_x\mathrm{Im}[\Pi_{+}^{\alpha}]|_{\omega=-q_x v_d^{\alpha}}, \tag{33}$$

where

$$|\bar{v}_i^{\alpha}(q_x;\omega)|^2 = \int dy_3 \bar{v}_{i\,+}^{\alpha}(q_x;a/2\hat{\mathbf{j}},\rho_3;\omega)\bar{v}_{i\,+}^{\alpha}(q_x;\rho_3,a/2\,\hat{\mathbf{j}};\omega)$$
$$\simeq \frac{2\pi\bar{e}^4}{|q_x|\,|\epsilon_{+}(q_x;\omega)|^2}|1 - v(q_x;a)\ \Pi_{+}^{\beta}|^2\ , \tag{34}$$

and $\bar{v}_{i\,\pm}^{\alpha}(q_x;\rho_3,\rho_2;\omega)$ is just the 2D Fourier transform of $\bar{v}_{i\,\pm}^{\alpha}(3;2)$ ($x_3 - x_2 \to q_x$, $t_3 - t_2 \to \omega$). In obtaining Eq. (34), we have already assumed that

$$\int d\rho_3\ \ \bar{v}_i^{\gamma}(q_x;\rho_1-\rho_3)|_{y_1=a/2,z_1=0}\delta(z_3)\bar{v}_i^{\gamma}(q_x;\rho_3-\rho_2)|_{y_2=a/2,z_2=0}$$
$$\gg \int d\rho_3\ \ \bar{v}_i^{\gamma}(q_x;\rho_1-\rho_3)|_{y_1=a/2,z_1=0}\ \delta(z_3)\ \bar{v}_i^{\gamma}(q_x;\rho_3-\rho_2)|_{y_2=-a/2,z_2=0} \tag{35}$$

since the modified Bessel function $K_0(x)$ [cf. Eq. (25)] goes to zero rapidly as x increases.

Furthermore, the frictional force acting on the electron system in the α wire, per unit mass and per unit length, due to the interaction with electrons in the β wire, is

$$F_{\alpha\beta} = -\frac{16\pi}{\hbar m^*} \sum_{q_{1x},k_x} \sum_{q_x} \sum_{n,m} \sum_{n',m'} C_{n,m}(q_x) C_{n',m'}(q_x) q_x \frac{|v(q_x;a)|^2}{|\epsilon_+(q_x;\omega)|^2} \times [f_\beta(\varepsilon_{m',q_{1x}+q_x}) - f_\beta(\varepsilon_{n',q_{1x}})][f_\alpha(\varepsilon_{m,k_x-q_x}) - f_\alpha(\varepsilon_{n,k_x})] \times [n_\alpha(\hbar\bar{\omega}) - n_\beta(\hbar\omega)]\delta[\bar{\omega} + \omega - q_x(v_d^\alpha - v_d^\beta)] , \quad (36)$$

with $\hbar\omega \equiv \varepsilon_{m',q_{1x}+q_x} - \varepsilon_{n',q_{1x}}$, $\hbar\bar{\omega} = \varepsilon_{m,k_x-q_x} - \varepsilon_{n,k_x}$ and $n_\gamma(\hbar\omega)$ is the Bose-Einstein distribution at lattice temperature. For weak electric fields, we may expand $\mathrm{Im}[\cdots]$ of Eq. (33) in $q_x v_d^\alpha$ and keep only the first-order term obtaining

$$F_{\alpha i} = \Omega_{\alpha i}\, v_d^\alpha , \quad (37)$$

with the momentum relaxation frequency per unit length due to impurity scattering, $\Omega_{\alpha i}$, given by

$$\Omega_{\alpha i} = -\frac{2n_i^{2D}\bar{e}^4}{m^*} \int dq_x \frac{|q_x|}{|\epsilon(q_x;0)|^2} \frac{\partial}{\partial\omega} \mathrm{Im}[\,\Pi_+^\alpha\,]|_{\omega=0} . \quad (38)$$

In the same manner, we may expand $\delta[\cdots]$ in Eq. (36) and obtain

$$F_{\alpha\beta} = \Omega_{\alpha\beta}(v_d^\alpha - v_d^\beta) \quad (39)$$

to first order in $(v_d^\alpha - v_d^\beta)$; the momentum relaxation frequency per unit length due to mutual Coulomb scattering, $\Omega_{\alpha\beta}$, is given by

$$\Omega_{\alpha\beta} = \frac{2\hbar^2}{m^* kT} \sum_{q_x} \int \frac{d\omega'}{2\pi} \frac{|q_x v(q_x;a)|^2}{|\epsilon_+(q_x;\omega')|^2} \times n(\hbar\omega')[\,1 + n(\hbar\omega')] \times \mathrm{Im}[\Pi_+^\alpha]\mathrm{Im}[\Pi_+^\beta(q_x;-\omega')] . \quad (40)$$

Thus Eqs. (10) and (11) reduce to

$$\frac{n^{1D}\bar{e}^2}{m^*} E = \bar{e}(\Omega_{\alpha i} + \Omega_{\alpha\beta})v_d^\alpha - \bar{e}\Omega_{\alpha\beta}v_d^\beta , \quad (41)$$

$$0 = \bar{e}\,(\Omega_{\beta i} + \Omega_{\beta\alpha})\, v_d^\beta - \bar{e}\,\Omega_{\beta\alpha}\, v_d^\alpha , \quad (42)$$

and the induced current I_i, is related to the external field E by $I_i = \sigma_{xx}^{\beta\alpha} E$ with the conductivities times length squared given as

$$\begin{pmatrix} \sigma_{xx}^{\alpha\alpha} \\ \sigma_{xx}^{\beta\alpha} \end{pmatrix} = \begin{pmatrix} \Omega_{\beta i} + \Omega_{\beta\alpha} \\ \Omega_{\beta\alpha} \end{pmatrix} \times \frac{(n^{1D}\,\bar{e})^2}{m^*[(\Omega_{\alpha i} + \Omega_{\alpha\beta})(\Omega_{\beta i} + \Omega_{\beta\alpha}) - \Omega_{\alpha\beta}\Omega_{\beta\alpha}]} . \quad (43)$$

III. NUMERICAL RESULTS AND DISCUSSION

We solve Eqs. (38) and (40) for GaAs quasi-1D wire with $\epsilon_\infty = 11$ and $m^* = 0.07m_0$. The two-dimensional electron density $n^{2D} = n^{1D}/w$, remains constant and it is taken to be 5×10^{11} cm^{-2}. The impurity density n_i^{2D} is equal to 1×10^{10}/cm^2. Furthermore, the width of the wire w relates to the confining frequency Ω through the approximate relation (8). As for the geometry of the two-wire system it is shown in Fig. 1. The electric field $\mathbf{E}$ is applied in wire α and the magnetic field $\mathbf{B}$ is along the z axis.

Figure 2 shows the magnetoconductivity in units of σ_0 (solid curve) and the conductivity ratio (dashed curve), with $\sigma_0 = e^2/\sqrt{2m^*\Delta} = 9.39 \times 10^{-13}$ C^{2}sec/kg m (Δ is taken to be 36.6 meV for convenience), as a function of magnetic field B. The confining frequency is 1 meV which corresponds to a wire width of 2687.5 Å and the wire separation is 200 Å. The temperature is taken to be 3 K. Both curves oscillate as function of the magnetic field. This is mainly due to the same oscillatory behavior of the momentum relaxation frequency, $\Omega_{\alpha i}$ for impurity scattering as shown in Fig. 2 since $\Omega_{\alpha i}$ (solid curve) is proportional to the derivative of the imaginary part of $\Pi_+^{(0)}$ which becomes[11] the density of states per unit length in the $q_x \to 0$ limit.

In Fig. 3, the momentum relaxation frequencies $\Omega_{\alpha i}$ (solid curve) and $\Omega_{\alpha\beta}$ (dashed curve) are plotted as function of the magnetic field. $\Omega_{\alpha\beta}$ is smaller than $\Omega_{\alpha i}$ by a factor of 10^6, both with respect to the absolute value and to the oscillation amplitude and its effect on the conductivity $\sigma_{xx}^{\alpha\alpha}$ is very small. It is verified in Fig. 4 in which $\sigma_{xx}^{\alpha i}/\sigma_0$ is plotted as function of B without taking into account the Coulomb interaction between wires. Thus, the oscillatory behavior of $\Omega_{\beta\alpha}$ has almost no effect on the conductivity ratio $\sigma_{xx}^{\beta\alpha}/\sigma_{xx}^{\alpha\alpha}$.

In Fig. 5, the conductivity ratio $\sigma_{xx}^{\beta\alpha}/\sigma_{xx}^{\alpha\alpha}$ (solid curve) and the conductivity $\sigma_{xx}^{\alpha\alpha}$ (dashed curve) are plotted as function of the wire separation d, cf. Fig. 1. The magnetic field is 2 T and the confining frequency 10 meV which corresponds to a wire width of 268.75 Å. The conductivity $\sigma_{xx}^{\alpha\alpha}$ varies almost linearly with d until $d = 148$ Å and saturates at about $d = 236$ Å; in other words, the wires are almost independent of each other

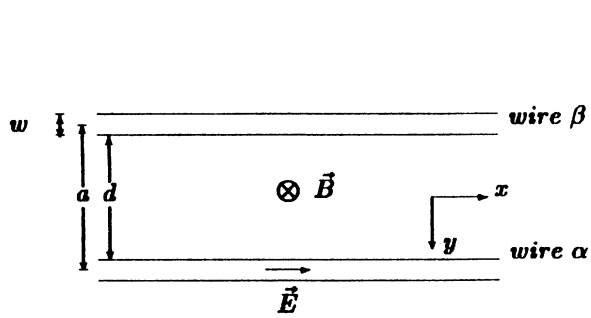

FIG. 1. The geometry of the two-wire system.

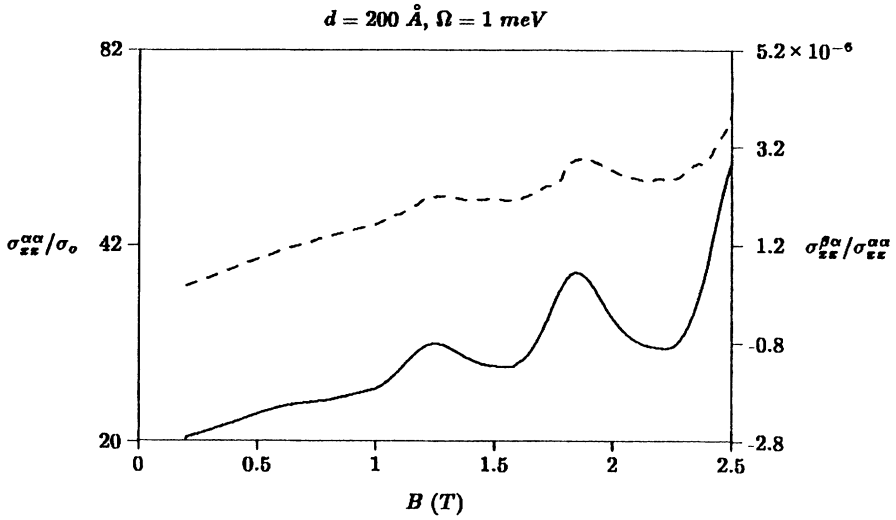

FIG. 2. Magnetoconductivity $\sigma_{xx}^{\alpha\alpha}/\sigma_0$ (solid curve) and conductivity ratio $\sigma_{xx}^{\beta\alpha}/\sigma_{xx}^{\alpha\alpha}$ (dashed curve) as function of the magnetic field for quantum wires with width $w = 2687.5$ Å and number density $n^{1D} = 1.34 \times 10^7$ cm^{-1} at temperature $T = 3$ K. The wire separation is 200 Å.

when the separation is more than 236 Å. On the other hand, the conductivity ratio decreases approximately, linearly with d for $d > 100$ Å. For $60 \leq d \leq 100$ Å, the conductivity ratio depends very little on the wire separation. However, for $d < 100$ Å the results are only indicative since particle exchange or tunneling between wires can occur for such a small separation. In this case, we cannot distinguish electrons from different wires and the Hamiltonian in Eq. (1) is likely not to be valid. In the opposite limit, i.e., for very large d (or a) Eq. (1) is valid and $\Omega_{\alpha\beta}$ decreases approximately as a^{-2}. This behavior of $\Omega_{\alpha\beta}$ can be understood from $\Omega_{\alpha\beta} \propto \int dq_x \, |v(q_x;a)|^2/|\epsilon_+(q_x;\omega')|^2$ as seen in Eq. (40). Now $v(q_x;a)$ goes as $e^{-q_x a}/\sqrt{q_x a}$ for large $q_x a$. Therefore, only the low-wave-number limit of the integrand dominates and $\epsilon_+(q_x;\omega)$, as given by Eq. (30), becomes

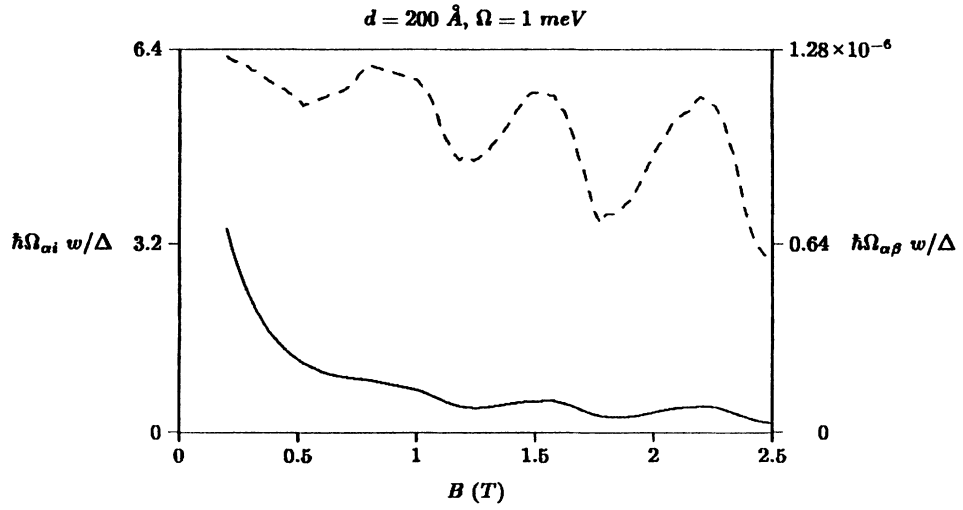

FIG. 3. Relaxation frequency per unit length due to impurity scattering $\hbar\Omega_{\alpha i}\, w/\Delta$ (solid curve) and due to Coulomb scattering between wires $\hbar\Omega_{\alpha\beta}\, w/\Delta$ (dashed curve) as function of the magnetic field for quantum wires with width $w = 2687.5$ Å and number density $n^{1D} = 1.34 \times 10^7$ cm^{-1} at temperature $T = 3$ K. The wire separation is 200 Å.

$$\epsilon_+(q_x;\omega) \sim -8e^4 \frac{q_x(a-w/2)}{x_c} \ln(x_c)\, \Pi_+^\alpha \Pi_+^\beta \qquad (44)$$

at low temperatures. For $a \gg w/2$, $\epsilon_+ \sim a$, or in other words, $\Omega_{\alpha\beta} \sim a^{-2}$ since $v(q_x;a)$ is independent of a at the low-wave-number limit, cf. Eq. (27).

This a^{-2} behavior of $\Omega_{\alpha\beta}$ is tied to the quasi-1D geometry of the two-electron system. Naturally, it raises the question about the relation of $\Omega_{\alpha\beta} = f(a)$ in, e.g., a 2D geometry and whether in such a geometry the current transfer ratio I_i/I_a is smaller or larger. As is immediately obvious I_i/I_a depends mainly on d (or a) and on the densities of the electron systems involved as Eq. (43) shows, all other parameters being the same for both systems. Below, for definiteness we compare $\Omega_{\alpha\beta}^{1D}$ and $\Omega_{\alpha\beta}^{2D}$ as well as the corresponding drag voltages V_D^{1D} and V_D^{2D}, for low temperatures when the energy transfer $\hbar\omega'$ in Eq. (40) is small, and the upper limit can be replaced by kT. In this case, Eq. (40), for zero magnetic field ($\tilde{m} = m^*$), can be written as

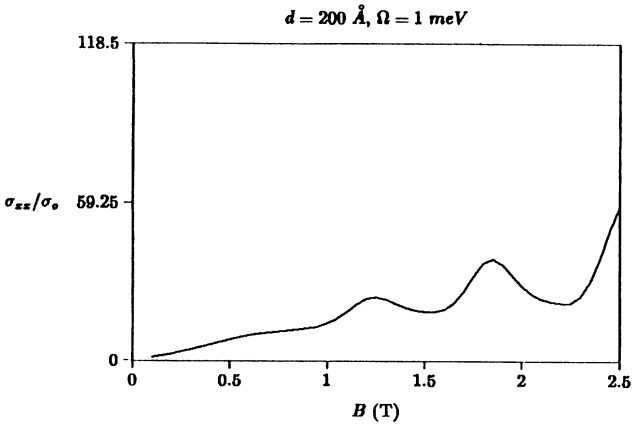

FIG. 4. Magnetoconductivity $\sigma_{xx}^{\alpha\alpha}/\sigma_0$ as function of the magnetic field for quantum wires with width w = 2687.5 Å and number density $n^{1D} = 1.34 \times 10^7$ cm^{-1} at temperature T = 3 K. Coulomb interaction between wires is absent.

$$\Omega_{\alpha\beta}^{1D} \sim \frac{4m^*}{\hbar^3} \sum_{q_x} \sum_{n,m,n',m'} \frac{|v(q_x;a)|^2}{|\epsilon_+^{1D}(q_x;0)|^2} (kT)^2 C_{n,m}(q_x) C_{n',m'}(q_x) \times \frac{\partial f_\alpha(\varepsilon_{k_x})}{\partial \varepsilon_{k_x}}\bigg|_{k_x = q_x/2 - (n-m)\tilde{m}\tilde{\omega}/\hbar q_x} \frac{\partial f_\beta(\varepsilon_{k_x})}{\partial \varepsilon_{k_x}}\bigg|_{k_x = q_x/2 - (n'-m')\tilde{m}\tilde{\omega}/\hbar q_x} . \qquad (45)$$

In the 2D case, the corresponding coupling frequency[12] per unit area is

$$\Omega_{\alpha\beta}^{2D} \sim \frac{4m^*}{\hbar^3} \sum_{q,k_\alpha,k_\beta} \frac{|v(q)|^2}{|\epsilon_+^{2D}(q;0)|^2} (kT)^2 |q| \frac{\partial f(\varepsilon_{k_\alpha})}{\partial \varepsilon_{k_\alpha}} \times \frac{\partial f(\varepsilon_{k_\beta})}{\partial \varepsilon_{k_\beta}} , \qquad (46)$$

where q, k_α, and k_β are the corresponding 2D wave vectors. Both frequencies show a quadratic dependence on temperature as expected for electron-electron interaction. As will be reported elsewhere[12] the corresponding numerical results show almost exactly the same T^2 dependence. Suppose now that the screened interactions $v(q_x;a)/\epsilon_+^{1D}(q_x;0)$ and $v(q)/\epsilon_+^{2D}(q;0)$ have the same

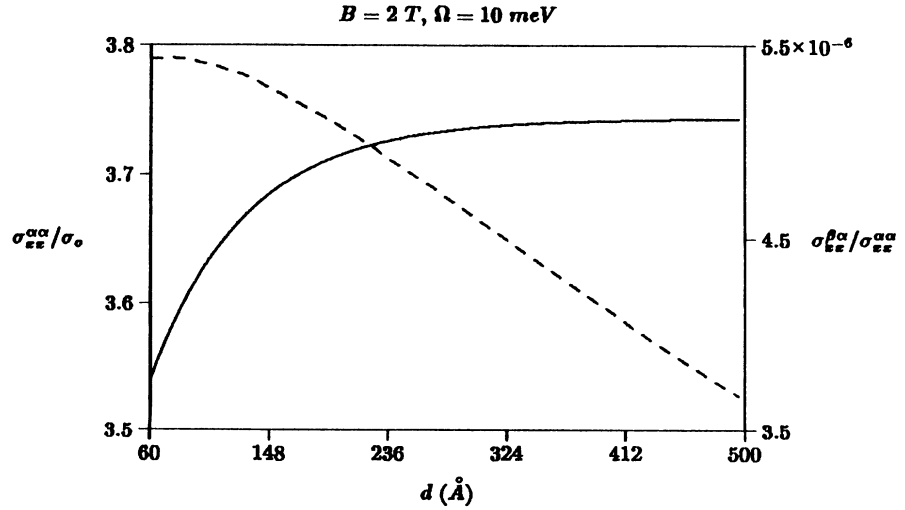

FIG. 5. Magnetoconductivity $\sigma_{xx}^{\alpha\alpha}/\sigma_0$ (solid curve) and conductivity ratio $\sigma_{xx}^{\beta\alpha}\sigma_{xx}^{\alpha\alpha}$ (dashed curve) as a function of the wire separation a for quantum wires with width w = 268.75 Å and number density $n^{1D} = 1.34 \times 10^6$ cm^{-1} at temperature T = 3 K. The magnetic field is 2 T.

strength which necessarily means different separation distances d. Then $\Omega_{\alpha\beta}^{1D}/\Omega_{\alpha\beta}^{2D} \sim 1/q_s^{2D}$ where q_s^{2D} is the screening wave number in the 2D electron gas. As a result, the ratio of the drag voltage V_D to the applied current I_a in the 1D case to that of the 2D case is obtained as

$$\frac{(V_D/I_a)^{1D}}{(V_D/I_a)^{2D}} = n^{2D}\Omega_{\alpha\beta}^{2D}/n^{1D}\Omega_{\alpha\beta}^{1D} \sim n^{2D}/n^{1D}q_s^{2D} \sim \hbar^2 n^{2D}/2m^*\bar{e}^2 n^{1D}. \quad (47)$$

Therefore, in this particular case the electron densities determine which drag will be stronger or weaker. A fuller comparison, with less approximations, will be reported elsewhere.[12]

IV. SUMMARY

In this paper we have derived coupled momentum-balance equations for electrons in coupled quasi-1D wires, in terms of the nonequilibrium number polarizability of electrons, in the presence of an external magnetic field. Mutual Coulomb interaction and Coulombic impurity scattering have been considered at low temperatures. A drifted-temperature model has been adopted to decouple the momentum balance equations for different wires. Screening of the electron-impurity interaction has been taken into account self-consistently (without vertex corrections) . Both the magnetoconductivity $\sigma_{xx}^{\alpha\alpha}$ and the conductivity ratio $\sigma_{xx}^{\beta\alpha}/\sigma_{xx}^{\alpha\alpha}$ exhibit Shubnikov–de Haas oscillations. The current ratio I_i/I_a and the relaxation frequency decrease slightly with wire separation $d \leq 100$ Å. For larger d they decrease almost linearly and for d much larger than the width they decrease as d^{-2}; this latter dependence reflects the corresponding d^{-1} dependence of the screened interaction which in two and three dimensions becomes[12] d^{-2} and d^{-3} leading to $\Omega_{\alpha\beta} \sim d^{-4}$ and $\Omega_{\alpha\beta} \sim d^{-6}$, respectively, as has been reported independently in Refs. 13 and 3.

ACKNOWLEDGMENTS

This work of both of us was supported by NSERC Grant No. URF0093498.

[1] P. J. Price, Physica **117B**, 750 (1983); C. Jacoboni and P. J. Price, Solid-State Electron **31**, 649 (1988); I. I. Boiko and Yu. M. Sirenko, Phys. Status Solidi B **159**, 805 (1990).
[2] P. M. Solomon, J. Price, D. J. Frank, and D. C. La Tulipe, Phys. Rev. Lett. **63**, 2508 (1989).
[3] B. Laikhtman and P. M. Solomon, Phys. Rev. B **41**, 9921 (1990).
[4] T. Oshima, M. Okada, M. Matsuda, N. Yokoyama, and A. Shibatomi, Superlattices Microstruct. **5**, 247 (1989); for additional pertinent works, see references in P. Vasilopoulos and F. M. Peeters, Phys. Rev. B **40**, 10079 (1989).
[5] M. L. Roukes, A. Sherer, S. J. Allen, Jr., H. G. Craighead, R. M. Ruthen, E. D. Beebe, and J. P. Harbison, Phys. Rev. Lett. **59**, 3011 (1987).
[6] K. F. Berggren, G. Roos, and H. Van Houten, Phys. Rev. B **37**, 10118 (1988).
[7] P. C. Martin and J. Schwinger, Phys. Rev. **115**, 1342 (1959).
[8] L. P. Kadanoff and G. Baym, *Quantum Statistical Mechanics* (Benjamin, New York, 1962).
[9] H. C. Tso, Ph.D. thesis, Stevens Institute of Technology, Hoboken, New Jersey, 1990.
[10] H. C. Tso and N. J. M. Horing, Phys. Rev. B **44**, 8886 (1991).
[11] H. C. Tso and P. Vasilopoulos, Phys. Rev. B **44**, 12952 (1991); T. Ando and Y. Murayama, J. Phys. Soc. Jpn. **54**, 1519 (1985).
[12] H. C. Tso and P. Vasilopoulos (unpublished).
[13] T. J. Gramila, J. Eisenstein, A. H. MacDonald, L. N. Pfeiffer, and K. W. West, Phys. Rev. Lett. **66**, 1216 (1991).